Molecular Biology of the Cell
Vol. 17, 4876–4887, November 2006

The Ca^{2+}-binding Protein ALG-2 Is Recruited to Endoplasmic Reticulum Exit Sites by Sec31A and Stabilizes the Localization of Sec31A[D]

Akinori Yamasaki,* Katsuko Tani,† Akitsugu Yamamoto,‡ Naomi Kitamura,* and Masayuki Komada*

*Department of Biological Sciences, Tokyo Institute of Technology, Yokohama 226-8501, Japan; †School of Life Science, Tokyo University of Pharmacy and Life Science, Hachioji 192-0392, Japan; and ‡Department of Bio-science, Nagahama Institute of Bio-science and Technology, Nagahama 526-0829, Japan

Submitted May 22, 2006; Revised August 8, 2006; Accepted August 29, 2006
Monitoring Editor: Randy Schekman

The formation of transport vesicles that bud from endoplasmic reticulum (ER) exit sites is dependent on the COPII coat made up of three components: the small GTPase Sar1, the Sec23/24 complex, and the Sec13/31 complex. Here, we provide evidence that apoptosis-linked gene 2 (ALG-2), a Ca^{2+}-binding protein of unknown function, regulates the COPII function at ER exit sites in mammalian cells. ALG-2 bound to the Pro-rich region of Sec31A, a ubiquitously expressed mammalian orthologue of yeast Sec31, in a Ca^{2+}-dependent manner and colocalized with Sec31A at ER exit sites. A Ca^{2+} binding-deficient ALG-2 mutant, which did not bind Sec31A, lost the ability to localize to ER exit sites. Overexpression of the Pro-rich region of Sec31A or RNA interference-mediated Sec31A depletion also abolished the ALG-2 localization at these sites. In contrast, depletion of ALG-2 substantially reduced the level of Sec31A associated with the membrane at ER exit sites. Finally, treatment with a cell-permeable Ca^{2+} chelator caused the mislocalization of ALG-2, which was accompanied by a reduced level of Sec31A at ER exit sites. We conclude that ALG-2 is recruited to ER exit sites via Ca^{2+}-dependent interaction with Sec31A and in turn stabilizes the localization of Sec31A at these sites.

INTRODUCTION

Newly synthesized secretory, plasma membrane, Golgi, and endosomal/lysosomal proteins are transported from the endoplasmic reticulum (ER) to the *cis*-Golgi compartment by vesicular transport. Initial vesicles that carry these cargo proteins are coated with the COPII complex and evaginate from specialized sites of the ER membrane referred to as ER exit sites. The vesicles are uncoated and destined for the *cis*-Golgi membrane via larger membranous intermediates referred to as the ER-Golgi intermediate compartment or vesicular-tubular cluster (for recent review, see Tang *et al*., 2005; Watson and Stephens, 2005).

The COPII coat of the ER-to-Golgi transport vesicles has been extensively studied in the yeast *Saccharomyces cerevisiae*. The coat consists of five principal components: Sar1, Sec23, Sec24, Sec13, and Sec31. Sar1 is a small GTPase of the Arf family, which is activated by the guanine nucleotide exchange activity of a transmembrane ER protein, Sec12 (Nakano and Muramatsu, 1989; Barlowe and Schekman, 1993). Exchange of Sar1-bound GDP to GTP induces the conformational change of Sar1 and triggers the recruitment of the Sec23–Sec24 complex to ER exit sites (Hicke *et al*., 1992; Matsuoka *et al*., 1998). Sec23 and Sec24, together with Sar1, form a prebudding "inner shell" complex, which binds to ER export signals in the cytoplasmic regions of cargo and their receptors and concentrates them at the sites of vesicle budding (Kuehn *et al*., 1998). The Sec23–Sec24 complex further recruits the Sec13–Sec31 complex (Salama *et al*., 1993; Matsuoka *et al*., 1998). The Sec13–Sec31 complex self-assembles to form the "outer shell" of the COPII coat and induces the membrane deformation at ER exit sites (Barlowe *et al*., 1994; Stagg *et al*., 2006). Sec23 is a GTPase-activating protein for Sar1 (Yoshihisa *et al*., 1993). Sec23-stimulated hydrolysis of Sar1-bound GTP to GDP results in the dissociation of the COPII coat from the transport vesicles, which allows the fusion of the vesicles with the ER-Golgi intermediate compartment.

The fundamental machinery for the formation of the ER-to-Golgi transport vesicles is conserved in mammalian cells. However, the COPII system is more diversified in mammals. Mammalian genomes encode multiple homologues for most of the COPII components: two for Sar1, two for Sec23, four for Sec24, and two for Sec31. Sec13 is the only component encoded by a single gene. For Sec31, two homologues, Sec31A and Sec31B, both of which function at ER exit sites, are present in mammals (Shugrue *et al*., 1999; Tang *et al*., 2000; Stankewich *et al*., 2006). Whereas Sec31A is widely

This article was published online ahead of print in *MBC in Press* (http://www.molbiolcell.org/cgi/doi/10.1091/mbc.E06–05–0444) on September 6, 2006.

[D] The online version of this article contains supplemental material at *MBC Online* (http://www.molbiolcell.org).

Address correspondence to: Masayuki Komada (makomada@bio.titech.ac.jp).

Abbreviations used: BAPTA-AM, 1,2-bis(2-amino phenoxy)ethane-*N*,*N*,*N*′,*N*′-tetraacetic acid-tetrakis acetoxymethyl ester; BFA, brefeldin A; ER, endoplasmic reticulum; GFP, green fluorescent protein; GST, glutathione *S*-transferase; LBPA, lysobisphosphatidic acid; MVB, multivesicular body; PCR, polymerase chain reaction; PEF, penta-EF-hand; RNAi, RNA interference; siRNA, small interfering RNA; Vps, vacuolar protein sorting; VSVG, vesicular stomatitis virus G protein.

expressed in various tissues, Sec31B is predominantly expressed in the testis (Tang *et al*., 2000). In addition, a number of splicing variants are reported for Sec31B (Stankewich *et al*., 2006). Whether the two Sec31 homologues have a redundant role or specific functions remains unknown. However, the presence of multiple homologues and splicing variants for Sec31 as well as for other COPII components, suggests greater complexity of the COPII system in the same or in different cell types in multicellular organisms.

Apoptosis-linked gene 2 (ALG-2) is a Ca^{2+}-binding protein that belongs to the penta-EF-hand (PEF) family of proteins with five tandem EF-hand motifs (Maki *et al*., 2002; Tarabykina *et al*., 2004). The binding of Ca^{2+} to ALG-2 induces a conformational change of the protein (Maki *et al*., 1998; Lo *et al*., 1999) that allows its interaction with other cytoplasmic proteins (Tarabykina *et al*., 2004). This suggests that ALG-2 serves as a Ca^{2+} sensor in Ca^{2+}-regulated cellular processes mediated by ALG-2–binding proteins. ALG-2 was identified as a protein, depletion of which by antisense RNA renders T-cell hybridoma cells resistant to apoptosis induced by a variety of apoptotic stimuli (Vito *et al*., 1996). However, the role of ALG-2 in apoptosis is largely unknown at a molecular level (Tarabykina *et al*., 2004). ALG-2 is also implicated in membrane trafficking at endosomes, because it binds in a Ca^{2+}-dependent manner to a class E vacuolar protein sorting (Vps) protein, ALG-2-interacting protein X (Alix) (Missotten *et al*., 1999; Vito *et al*., 1999). Alix is essential for the biogenesis of multivesicular bodies (MVBs), a subpopulation of endosomes with multiple lumenal vesicles (Matsuo *et al*., 2004). It is further required for the budding of enveloped viruses from infected cells, a process that is topologically equivalent to the formation of the internal vesicles of MVBs (Strack *et al*., 2003; von Schwedler *et al*., 2003). However, whether ALG-2 is involved in these processes via interaction with Alix is unclear as well.

Experiments using semiintact and living cells have implicated Ca^{2+} in various stages of the vesicular traffic pathway between the ER and the Golgi. They include the late targeting/fusion step of the ER-to-Golgi anterograde traffic (Beckers and Balch, 1989; Pind *et al*., 1994; Chen *et al*., 2002), the Golgi-to-ER retrograde traffic (Ivessa *et al*., 1995; Chen *et al*., 2002), and the stabilization of the COPI coat (Ahluwalia *et al*., 2001). However, the molecular mechanisms underlying the Ca^{2+}-mediated regulation are poorly understood. In this study, we demonstrate that ALG-2 localizes to ER exit sites via Ca^{2+}-dependent interaction with Sec31A and is required for maintaining normal Sec31A levels at these sites, thus providing a novel molecular basis for the regulation of the COPII coat function by Ca^{2+}.

MATERIALS AND METHODS

cDNA Expression Constructs and Transfection

The FLAG-tagged mammalian expression vectors for human ALG-2 and its mutant ALG-$2^{E47/114A}$ (Shibata *et al*., 2004) were provided by Drs. M. Maki and H. Shibata (Nagoya University, Nagoya, Japan). The hemagglutinin (HA)-tagged expression vectors for these proteins were constructed by amplifying their cDNAs using polymerase chain reaction (PCR) and inserting into pME-HA (Mizuno *et al*., 2003). The human Sec31A cDNA was excised from pFLAG-CMV-6B-Sec31A and cloned into pME-FLAG (Mizuno *et al*., 2003) to construct the FLAG-Sec31A expression vector. The cDNAs for the truncated mutants of Sec31A were amplified by PCR from pFLAG-CMV-6B-Sec31A and cloned into pME-FLAG. The expression vectors for green fluorescent protein (GFP)-tagged Sar1a mutants, $Sar1^{H79G}$ and $Sar1^{T39N}$, were constructed by inserting their cDNAs (Shimoi *et al*., 2005) into pEGFP-C1 (Clontech, Mountain View, CA). The cDNA for human Alix was amplified by PCR from pGFP-Alix (Shibata *et al*., 2004; provided by Drs. Maki and Shibata) and cloned into pEGFP-N1 (Clontech) to construct the expression vector for Alix, which is tagged at the C terminal with green fluorescent protein (GFP). The sequences of PCR-amplified cDNAs were verified by DNA sequencing. Vectors were transfected into cells for 2 d by using the FuGENE 6 transfection reagent (Roche Diagnostics, Indianapolis, IN).

RNA Interference (RNAi)

Using the small interfering RNA (siRNA) expression vector pSilencer 1.0-U6 (Ambion, Austin, TX), vectors that target human ALG-2 and Sec31A mRNAs were constructed. The ALG-2 siRNA vectors A-siRNA1 and A-siRNA2 target the nucleotide residues at positions 474-492 in the coding region (5′-GCAGAGGTTGACGGATATA-3′) and 869-887 in the 3′ noncoding region (5′-AGATGTCTCTGGTTCTATA-3′) relative to the translation initiation codon, respectively. The Sec31A siRNA vectors S-siRNA1 and S-siRNA2 target the nucleotide residues 872-890 (5′-ACACAGGAGAGGTGTTATA-3′) and 907-925 (5′-ACACAGTGGTGCTTCGATA-3′) from the translation initiation codon, respectively. These vectors and the empty control vector were transfected into HeLa cells twice at 48-h intervals. To express Alix-GFP in these cells, its expression vector was cotransfected with the siRNA vectors in the second round of transfection.

Anti-ALG-2 Antibody

A full-length cDNA for mouse ALG-2 was cloned in-frame into the vector pGEX6P-2 (GE Healthcare, Little Chalfont, Buckinghamshire, United Kingdom) to generate a glutathione *S*-transferase (GST) fusion construct. The GST-ALG-2 fusion protein was purified from transformed *Escherichia coli* strain BL21 by using glutathione-Sepharose affinity beads (GE Healthcare), and 200 μg of the protein was used to immunize each rabbit. Antisera were collected by standard procedures.

Immunoprecipitation and Immunoblotting

Cell lysates were prepared by solubilizing cells with lysis buffer (20 mM Tris-HCl, pH 7.4, 150 mM KCl, 10 mM 3-[(3-cholamidopropyl)dimethylammonio]-1-propanesulfonic acid, 1 mM phenylmethylsulfonyl fluoride, 2 μg/ml aprotinin, 1 μg/ml leupeptin, and 1 μg/ml pepstatin A) for 30 min and collecting the supernatants after centrifugation at 12,000 $\times$ *g* for 15 min. The lysates were used directly for immunoblotting, or immunoprecipitated with 5 μl of anti-ALG-2, 4 μg of anti-FLAG (Sigma-Aldrich, St. Louis, MO), or 2 μg of anti-HA (Sigma-Aldrich) antibody. The immunoblot analysis was performed according to standard procedures. Primary antibodies used were anti-ALG-2 (1:200), 1 μg/ml anti-Sec31A (BD Biosciences Transduction Laboratories, Lexington, KY), anti-Sec13 (1:1000; Tang *et al*., 1997; provided by Dr. W. Hong, Institute of Molecular and Cell Biology, Singapore, Republic of Singapore), 4 μg/ml anti-FLAG (Sigma-Aldrich), 0.4 μg/ml anti-HA (Sigma-Aldrich), anti-α-tubulin (1:8000; Sigma-Aldrich), 0.4 μg/ml anti-transcription factor TF-IID (Santa Cruz Biotechnology, Santa Cruz, CA), 0.4 μg/ml anti-phospholipase Cγ (Santa Cruz Biotechnology), and 0.5 μg/ml anti-epidermal growth factor receptor (MBL, Nagoya, Japan) antibodies. Secondary antibodies were peroxidase-conjugated anti-mouse IgG and anti-rabbit IgG antibodies (GE Healthcare). Blots were detected using the ECL reagent (GE Healthcare). To quantify the intensity of bands in immunoblot membranes, the NIH Image analysis program ImageJ was used (http://rsb.info.nih.gov/ij/).

GST Pull-Down and Mass Spectrometry

HeLa cells in a 90-mm dish were lysed with 0.8 ml of lysis buffer; and the supernatant, after centrifugation at 12,000 $\times$ *g*, was incubated with 1 μg of GST or GST-ALG-2 immobilized on glutathione beads for 16 h at 4°C. Ca^{2+} (1 mM) or 5 mM EGTA was added to the lysate before incubation with the GST-fusion protein. After the beads had been washed three times, bound proteins were eluted with boiling SDS-PAGE sample buffer, separated by SDS-PAGE, visualized by silver staining (Silver Stain MS kit; Wako Pure Chemicals, Osaka, Japan), and excised from the gel. In-gel digestion with trypsin followed by an analysis using UltraFlex matrix-assisted laser desorption ionization/time of flight mass spectrometry (Bruker Daltonics, Billerica, MA) was performed according to the manufacturer's instructions. Data were analyzed using the MASCOT search program (Matrix Science, Boston, MA).

Immunofluorescence Staining

HeLa cells were fixed with 4% paraformaldehyde in phosphate-buffered saline on ice for 10 min, permeabilized with 0.2% Triton X-100 in phosphate-buffered saline, and stained with rabbit polyclonal anti-ALG-2 (1:1000), 0.25 μg/ml mouse monoclonal anti-Sec31A (BD Biosciences Transduction Laboratories), mouse monoclonal anti-p125 (1:250; Shimoi *et al*., 2005), rabbit polyclonal anti-β-COP (1:300; Shimoi *et al*., 2005), 1.6 μg/ml mouse monoclonal anti-FLAG (Sigma-Aldrich), 0.4 μg/ml rabbit polyclonal anti-FLAG (Sigma-Aldrich), rat monoclonal anti-GFP (1:1000; Nacalai Tesque, Kyoto, Japan), or 4 μg/ml rabbit polyclonal anti-GFP (Invitrogen, Carlsbad, CA) antibody by using standard procedures. Secondary antibodies were Alexa488-, 546-, 594-, and 633-conjugated anti-mouse IgG, anti-rabbit IgG, and anti-rat IgG antibodies (Invitrogen). Treatments with brefeldin A (BFA), 1,2-bis(2-amino phenoxy)ethane-*N*,*N*,*N*′,*N*′-tetraacetic acid-tetrakis acetoxymethyl ester (BAPTA-AM), and A23187 were performed by incubating cells with 5 μg/ml BFA

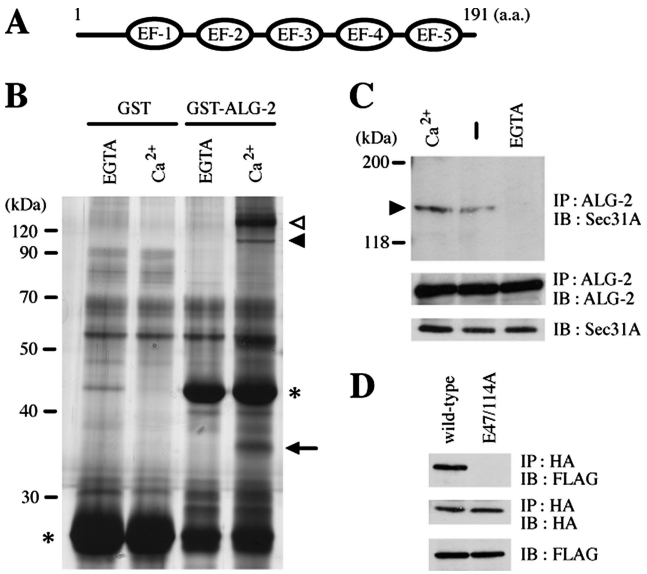

Figure 1. ALG-2 binds Sec31A in a Ca^{2+}-dependent manner. (A) Schematic structure of ALG-2. Positions of the five EF-hand motifs are indicated. (B) HeLa cell lysate was incubated with GST or GST-ALG-2 in the presence of EGTA or Ca^{2+}. Proteins pulled down by the GST proteins were separated by SDS-PAGE and visualized by silver staining. Open and closed arrowheads indicate Sec31A and Alix, respectively. An arrow indicates an unidentified protein. Asterisks indicate GST and GST-ALG-2 used for the pull down. (C) HeLa cell lysate was immunoprecipitated with anti-ALG-2 antibody in the presence of EGTA or Ca^{2+}, or in their absence, and immunoblotted with anti-Sec31A (top) or anti-ALG-2 (middle) antibody. The level of Sec31A expression was assessed by immunoblotting of the total cell lysate with anti-Sec31A antibody (bottom). (D) HeLa cells were transfected with HA-tagged wild-type ALG-2 or ALG-$2^{E47/114A}$ together with FLAG-tagged Sec31A. Lysates of the cells were immunoprecipitated with anti-HA antibody in the presence of Ca^{2+} and immunoblotted with anti-FLAG (top) or anti-HA (middle) antibody. The level of FLAG-Sec31A expression was assessed by immunoblotting of the total cell lysate with anti-FLAG antibody (bottom).

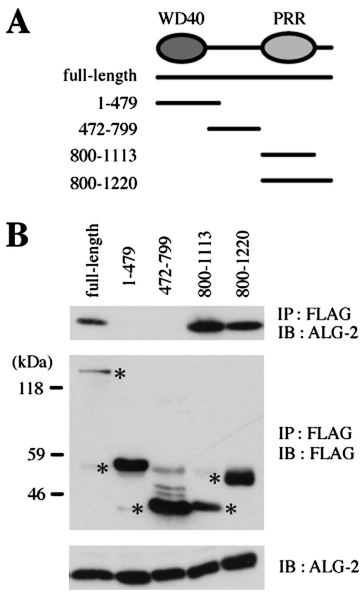

Figure 2. ALG-2 binds to the Pro-rich region of Sec31A. (A) Domain structure of Sec31A and the truncated mutants used in this study. The positions of the WD40 repeat domain (WD40) and the Pro-rich region (PRR) are indicated. (B) Lysates of HeLa cells transfected with FLAG-tagged full-length Sec31A or truncated mutants were immunoprecipitated with anti-FLAG antibody and immunoblotted with anti-ALG-2 (top) or anti-FLAG (middle) antibody. The expression level of endogenous ALG-2 was assessed by immunoblotting of the total cell lysate with anti-ALG-2 antibody (bottom). Asterisks indicate the positions of the Sec31A constructs (middle).

(Sigma-Aldrich) for 30 min, 25 μM BAPTA-AM (Nacalai Tesque) for 30 min, and 1 μM A23187 (Sigma-Aldrich) for 20 min, respectively, at 37°C. Fluorescence images were captured with a confocal microscope (Axiovert 200M; Carl Zeiss, Oberkochen, Germany) by using the LSM5 PASCAL system (Carl Zeiss).

Subcellular Fractionation

HeLa cells were homogenized by a Potter homogenizer in 10 mM Tris-HCl, pH 7.4, containing 1 mM phenylmethylsulfonyl fluoride, 2 μg/ml aprotinin, 1 μg/ml leupeptin, and 1 μg/ml pepstatin A, and then they were centrifuged at 1000 $\times$ *g* for 5 min at 4°C. The pellet was collected as the nuclear fraction and solubilized with the SDS-PAGE sample buffer. The supernatant (postnuclear fraction) was further centrifuged at 105,000 $\times$ *g* for 1 h at 4°C. The supernatant was recovered as the cytoplasmic fraction. The pellet (membrane fraction) was solubilized with the SDS-PAGE sample buffer. Proteins in each fraction, recovered from an equal amount of cells, were analyzed by immunoblotting.

RESULTS

ALG-2 Binds Sec31A in a Ca^{2+}-dependent Manner

To elucidate the Ca^{2+}-regulated function of the PEF family protein ALG-2 (Figure 1A), we tried to identify proteins that bind ALG-2 in a Ca^{2+}-dependent manner. ALG-2 was expressed as a GST-fusion protein in *E. coli*, immobilized on glutathione beads, and incubated with HeLa cell lysate in the presence of 1 mM Ca^{2+} or 5 mM EGTA. After the beads were washed, bound proteins were separated by SDS-PAGE and visualized by silver staining. A ~140-kDa protein was coprecipitated as a major ALG-2-binding protein in the presence of Ca^{2+} but not EGTA (Figure 1B, open arrowhead). It did not bind GST alone in the presence of EGTA or Ca^{2+} (Figure 1B). To identify the protein, the band was excised from the gel, digested with trypsin, and analyzed by mass spectrometry by using peptide mass finger printing. With a high probability, the protein was identified as Sec31A (MASCOT score = 177; Supplemental Figure S1). In addition, ~110-kDa and ~35-kDa proteins were also coprecipitated with GST-ALG-2 in a Ca^{2+}-dependent manner (Figure 1B, closed arrowhead and arrow). The ~110-kDa protein was identified as a known ALG-2-binding protein, Alix, by peptide mass finger printing (MASCOT score = 237; our unpublished data), verifying the reliability of the experiments. The identity of the ~35-kDa protein is currently unknown. Although its size is similar to that of Sec13, a binding partner of Sec31A, the mass spectrometric analysis provided no evidence that it is Sec13 (our unpublished data).

To confirm the interaction between ALG-2 and Sec31A within cells, we raised a rabbit polyclonal anti-ALG-2 antiserum and performed coimmunoprecipitation experiments. Endogenous ALG-2 was immunoprecipitated from HeLa cells by using anti-ALG-2 antibody in the presence of exogenously added Ca^{2+} or EGTA, or in their absence, and the precipitated proteins were immunoblotted with anti-Sec31A antibody. Anti-ALG-2 antibody coprecipitated endogenous Sec31A in the absence of Ca^{2+} and EGTA (Figure 1C, top, arrowhead). Addition of 10 μM Ca^{2+} during the immunoprecipitation increased the level of coprecipitated Sec31A,

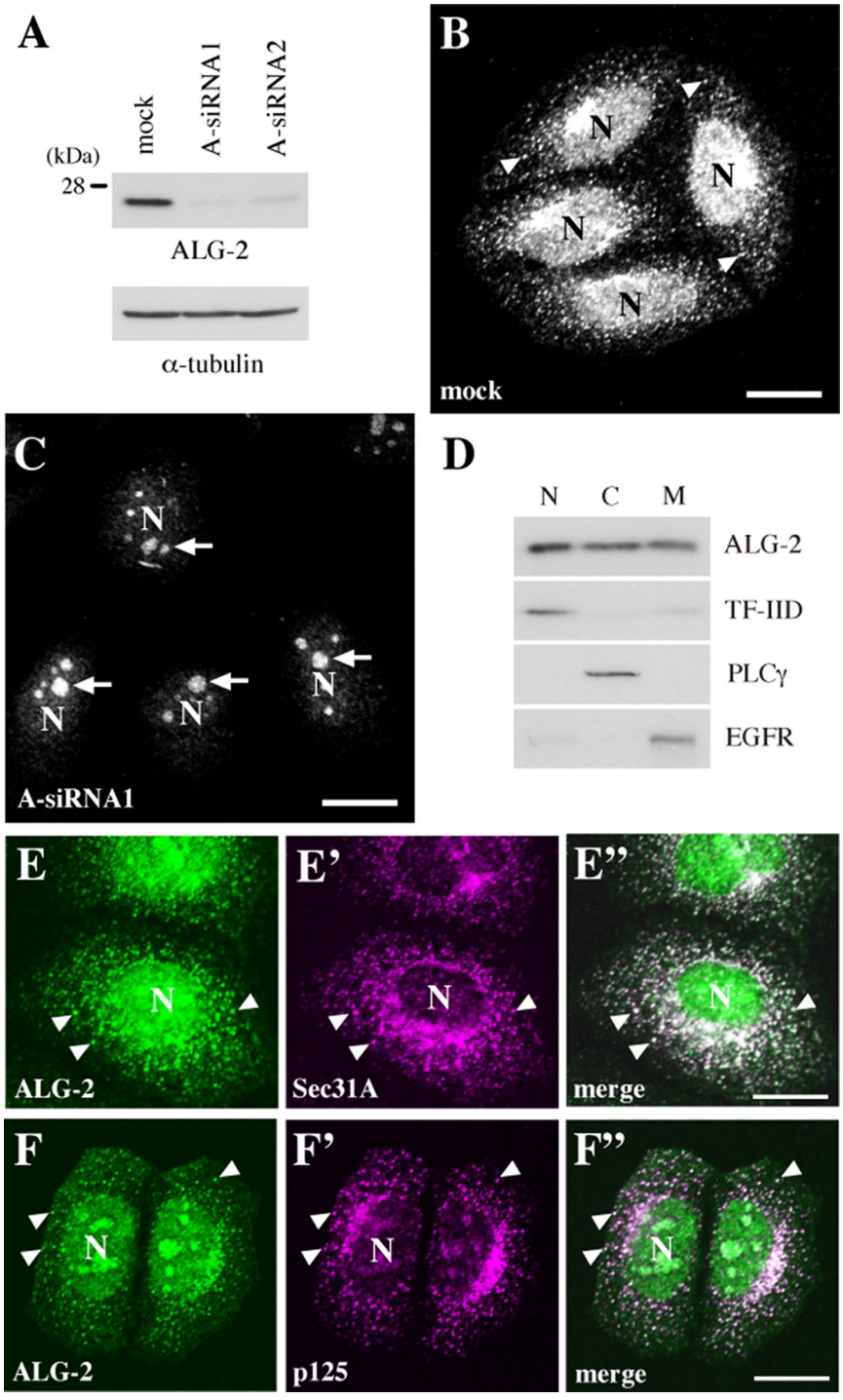

Figure 3. ALG-2 localizes to ER exit sites. (A) Lysates of HeLa cells transfected with the mock or ALG-2 siRNA expression vectors, A-siRNA1 and A-siRNA2, were immunoblotted with anti-ALG-2 (top) and anti-α-tubulin (bottom) antibodies. (B and C) Immunofluorescence staining of HeLa cells transfected with the mock (B) or A-siRNA1 (C) vector with anti-ALG-2 antibody. Arrowheads in B indicate typical ALG-2-positive punctate structures. Arrows in C indicate nonspecific staining of nucleoli in ALG-2-depleted cells. N indicates nuclei. Bars, 20 μm. (D) HeLa cells were homogenized and fractionated into nuclear (N), cytoplasmic (C), and membrane (M) fractions. Proteins in each fraction were immunoblotted with antibodies against ALG-2, TF-IID, phospholipase Cγ (PLCγ), and epidermal growth factor receptor (EGFR). (E–F″) HeLa cells were immunostained with anti-ALG-2 antibody (E and F) together with anti-Sec31A (E′) or anti-p125 (F′) antibody. E″ and F″ are merged images. Arrowheads indicate colocalization of ALG-2 with Sec31A (E–E″) and p125 (F–F″). N indicates nuclei. Bars, 20 μm.

whereas addition of 5 mM EGTA abolished the Sec31A interaction with ALG-2 (Figure 1C, top).

ALG-2$^{E47/114A}$ is a mutant in which the Glu residues at positions 47 and 114 in the first and third EF-hand motifs of ALG-2, respectively, are replaced by Ala. This mutant lacks Ca^{2+}-binding ability (Lo *et al.*, 1999). To further confirm that the interaction between ALG-2 and Sec31A is Ca^{2+} dependent, we examined the binding of ALG-2$^{E47/114A}$ to Sec31A. HA-tagged wild-type ALG-2 or ALG-2$^{E47/114A}$ was cotransfected with FLAG-tagged Sec31A into HeLa cells and immunoprecipitated with anti-HA antibody in the presence of 10 μM Ca^{2+}. Immunoblotting of the precipitates with anti-FLAG antibody showed that ALG-2$^{E47/114A}$ lacks Sec31A-binding ability (Figure 1D, top). Like endogenous ALG-2, HA-tagged wild-type ALG-2 was able to bind Sec31A (Figure 1D, top).

ALG-2 Binds to the Pro-rich Region of Sec31A

The structure of Sec31A can be divided into four parts: the N-terminal WD40 repeat domain (amino acids 1-322), the intervening region (323-807), the Pro-rich region (808-1145), and the C-terminal region (1146-1262) (amino acid numbers

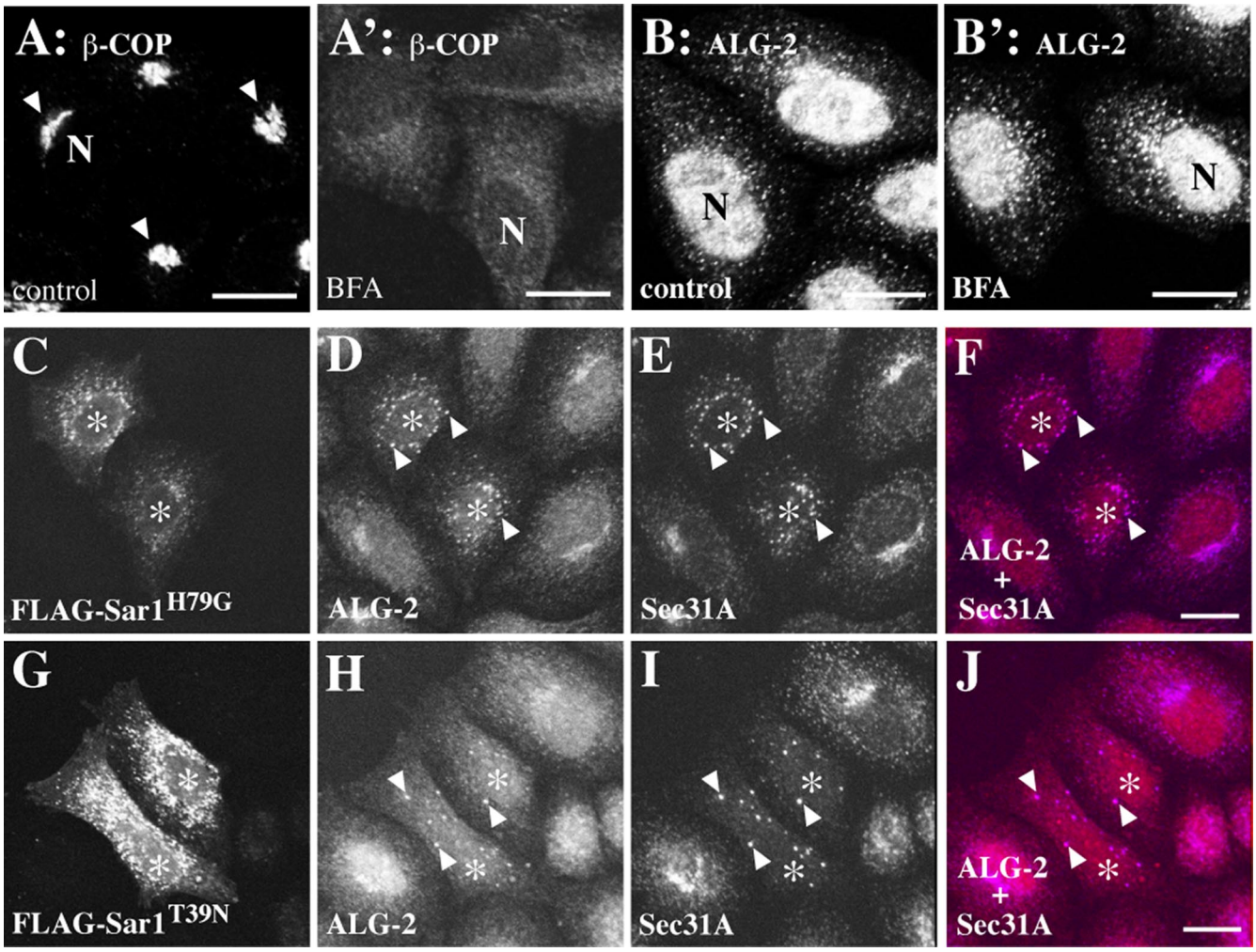

Figure 4. Effects of BFA treatment and Sar1 inhibition on ALG-2 localization. (A–B′) HeLa cells treated without (A and B) or with (A′ and B′) BFA were immunostained with anti-β-COP (A and A′) or anti-ALG-2 (B and B′) antibody. Arrowheads in A indicate the *cis*-Golgi region. N indicates the position of nuclei. (C–J) HeLa cells were transfected with GFP-tagged Sar1^{H79G} (C–F) or Sar1^{T39N} (G–J), and double stained with anti-ALG-2 (D and H; Alexa546) and anti-Sec31A (E and I; Alexa633) antibodies. C and G show the fluorescence of GFP-tagged Sar1 mutants. F and J are merged images of D + E and H + I, respectively. Asterisks indicate cells overexpressing Sar1^{H79G} (C–F) and Sar1^{T39N} (G–J). Arrowheads in D–F and H–J indicate colocalization of ALG-2 and Sec31A on morphologically aberrant structures. Bars, 20 μm.

for rat Sec31A; Shugrue *et al*., 1999). To roughly determine the ALG-2-binding region in Sec31A, four truncated mutants encompassing amino acids 1-479, 472-799, 800-1113, and 800-1220 of human Sec31A were constructed (Figure 2A). These mutants were tagged with the FLAG epitope, expressed in HeLa cells and immunoprecipitated with anti-FLAG antibody in the presence of 10 μM Ca^{2+}. Immunoblotting of the precipitates with anti-ALG-2 antibody showed that Sec31A$^{800\text{-}1113}$ and Sec31A$^{800\text{-}1220}$ bind ALG-2, whereas Sec31A$^{1\text{-}479}$ and Sec31A$^{472\text{-}799}$ do not. These results suggested that ALG-2 binds to the Pro-rich region between amino acids 800 and 1113 of Sec31A.

ALG-2 Localizes to Cytoplasmic Puncta

The subcellular localization site(s) of ALG-2 has been controversial (Tarabykina *et al*., 2004). We therefore examined it by immunofluorescence staining using our anti-ALG-2 antibody. To evaluate the specificity of the staining, we used RNAi-mediated ALG-2–depleted cells as a negative control. We generated two siRNA-expression vectors for human ALG-2 (A-siRNA1 and A-siRNA2), which could efficiently reduce the level of endogenous ALG-2 in HeLa cells as assessed by immunoblotting (Figure 3A).

We then stained HeLa cells transfected with the mock or ALG-2 siRNA vectors by using anti-ALG-2 antibody. In mock-transfected cells, the antibody stained numerous puncta scattered in the cytoplasm (Figure 3B, arrowheads). No such structures were observed in ALG-2 siRNA1- or siRNA2-transfected cells (Figure 3C; our unpublished data), indicating that the punctate staining by anti-ALG-2 in mock-transfected cells represents the distribution of ALG-2 and not background staining. In addition, staining of nuclei was observed in mock- but not in ALG-2 siRNA-transfected cells (Figure 3, B and C), indicating that ALG-2 is also present in the nucleus as reported previously (Kitaura *et al*., 2001).

To examine whether ALG-2 is associated with the membrane on the cytoplasmic puncta, we performed subcellular fractionation experiments. HeLa cells were homogenized in the absence of Ca^{2+} and EGTA, and separated into nuclear, cytoplasmic, and membrane fractions. Immunoblotting of the proteins in each fraction with anti-ALG-2 antibody showed that ALG-2 is distributed to the membrane fraction

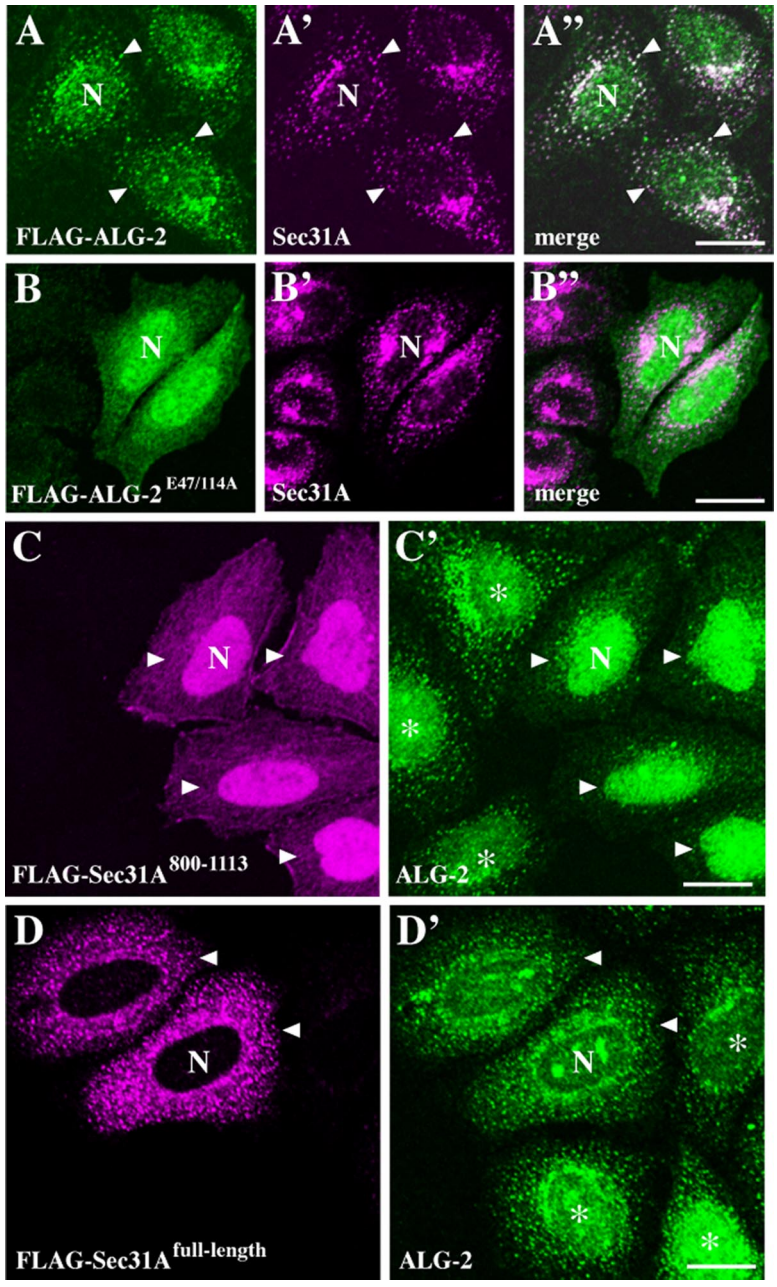

Figure 5. Localization of ALG-2 requires Ca^{2+} and the Pro-rich region of Sec31A. (A–B″) HeLa cells were transfected with FLAG-tagged wild-type ALG-2 (A–A″) or ALG-$2^{E47/114A}$ (B–B″), and double stained with anti-FLAG (A and B) and anti-Sec31A (A′ and B′) antibodies. A″ and B″ are merged images. Arrowheads indicate colocalization of FLAG-ALG-2 with Sec31A. (C–D′) HeLa cells were transfected with FLAG-tagged $Sec31A^{800-1113}$ (C and C′) or full-length Sec31A (D and D′), and double stained with anti-FLAG (C and D) and anti-ALG-2 (C′ and D′) antibodies. Arrowheads and asterisks indicate transfected and untransfected cells, respectively. N indicates nuclei. Bars, 20 μm.

as well as to the other fractions (Figure 3D, top), suggesting that the ALG-2–positive puncta are a membranous organelle. The nuclear distribution of ALG-2 was consistent with the nuclear staining of cells with anti-ALG-2 antibody (Figure 3B). The integrity of each fraction was verified by immunoblotting with antibodies against the transcription factor TF-IID, phospholipase Cγ, and epidermal growth factor receptor (Figure 3D).

ALG-2 Localizes to ER Exit Sites

The cytoplasmic punctate distribution of ALG-2 was reminiscent of that of ER exit sites where the ALG-2–binding partner Sec31A localizes (Shugrue *et al.*, 1999; Tang *et al.*, 2000). We therefore double stained HeLa cells with anti-ALG-2 and anti-Sec31A antibodies. Endogenous ALG-2 and Sec31A almost completely colocalized on the cytoplasmic puncta (Figure 3, E–E″). We also stained cells with antibody against p125, a protein of the phosphatidic acid-preferring phospholipase A_1 family that exclusively localizes to ER exit sites via interaction with Sec23 (Tani *et al.*, 1999; Shimoi *et al.*, 2005). The localization of endogenous ALG-2 and p125 also overlapped significantly (Figure 3, F–F″).

To confirm the ALG-2 localization at ER exit sites, we examined its distribution in HeLa cells treated with BFA, which induces the redistribution of COPI coat proteins from the Golgi to the ER without affecting the morphology of ER exit sites or the localization of COPII components at the sites (Klausner *et al.*, 1992; Ward *et al.*, 2001). Whereas the COPI component β-COP was detected broadly in cytoplasmic structures (most likely the ER) after treatment with 5 μg/ml BFA for 30 min (Figure 4, A and A′), the punctate pattern of ALG-2 localization was unaffected (Figure 4, B and B′). We

next examined the effects of overexpressing constitutively active (GTP-locked) and inactive (GDP-locked) Sar1 mutants, Sar1^{H79G} and Sar1^{T39N}, respectively, on the localization of ALG-2. Overexpression of Sar1^{H79G} causes clustering of the COPII component-associated ER membranes at perinuclear regions (Ward *et al*., 2001). In HeLa cells overexpressing GFP-tagged Sar1^{H79G}, endogenous ALG-2 and Sec31A colocalized on puncta with a clustered morphology (Figure 4, C–F, arrowheads). In cells overexpressing Sar1^{T39N}, by contrast, Sec31A is mostly excluded from the peripheral puncta and perinuclear structures, but found in several large spherical structures in the cytoplasm (Forster *et al*., 2006). In cells overexpressing GFP-tagged Sar1^{T39N}, ALG-2 colocalized with Sec31A on such spherical structures (Figure 4, G–J, arrowheads). Together, the results shown in Figure 4 confirmed the localization of ALG-2 at ER exit sites.

Ca^{2+}-dependent Sec31A Binding Is Required for the ALG-2 Localization to ER Exit Sites

To test whether the localization of ALG-2 to ER exit sites is mediated by Ca^{2+}-dependent interaction with Sec31A, we first examined the localization of FLAG-tagged wild-type ALG-2 and its Ca^{2+}-binding–deficient mutant ALG-2$^{E47/114A}$ in transfected HeLa cells. Wild-type ALG-2 largely colocalized with endogenous Sec31A on cytoplasmic puncta (Figure 5, A–A″). By contrast, ALG-2$^{E47/114A}$ was never detected on punctate Sec31A-positive structures (Figure 5, B–B″).

ALG-2 binds to the Pro-rich region of Sec31A (Figure 2B). We therefore asked whether the overexpression of the Pro-rich region alone affects the ALG-2 localization in a dominant-negative manner. When expressed in HeLa cells, FLAG-tagged Sec31A$^{800\text{-}1113}$, consisting solely of the Pro-rich region (Figure 2A), was distributed in the nucleus and cytoplasm (Figure 5C, arrowheads). In these cells, endogenous ALG-2 was significantly excluded from ER exit sites and instead detected at higher levels in the nucleus (Figure 5C′). By contrast, full-length Sec31A, when expressed at similar levels, colocalized with ALG-2 on cytoplasmic puncta and exhibited no effect on the ALG-2 localization (Figure 5, D and D′, arrowheads).

Finally, we examined the effect of RNAi-mediated depletion of Sec31A on the localization of ALG-2. We constructed two siRNA expression vectors for human Sec31A (S-siRNA1 and S-siRNA2) that, when expressed in HeLa cells, almost completely depleted endogenous Sec31A as assessed by immunoblotting (Figure 6A, top). When S-siRNA1– and S-siRNA2–transfected cells were double stained with anti-ALG-2 and anti-Sec31A antibodies, the cytoplasmic punctate staining for ALG-2 was mostly abolished in Sec31A-depleted cells (Figure 6, B and B′, asterisks; our unpublished data). In Figure 6, B and B′, we show a field where both Sec31A-depleted and undepleted cells are present to facilitate a side-by-side comparison. It should be noted, however, that ~80–90% of the siRNA-transfected cells exhibited undetectable level of anti-Sec31A staining (our unpublished data), which was consistent with the results of immunoblotting (Figure 6A). Immunoblotting showed that the cellular level of ALG-2 is unchanged by Sec31A depletion (Figure 6A, middle).

ALG-2 Stabilizes the Sec31A Localization at ER Exit Sites

We next examined whether ALG-2 plays a role in regulating the subcellular localization of Sec31A by using cells depleted of ALG-2 with RNAi. HeLa cells were transfected with A-siRNA1 or A-siRNA2 and double stained with anti-Sec31A and anti-ALG-2 antibodies. The level of anti-Sec31A staining was substantially reduced in ALG-2–depleted cells

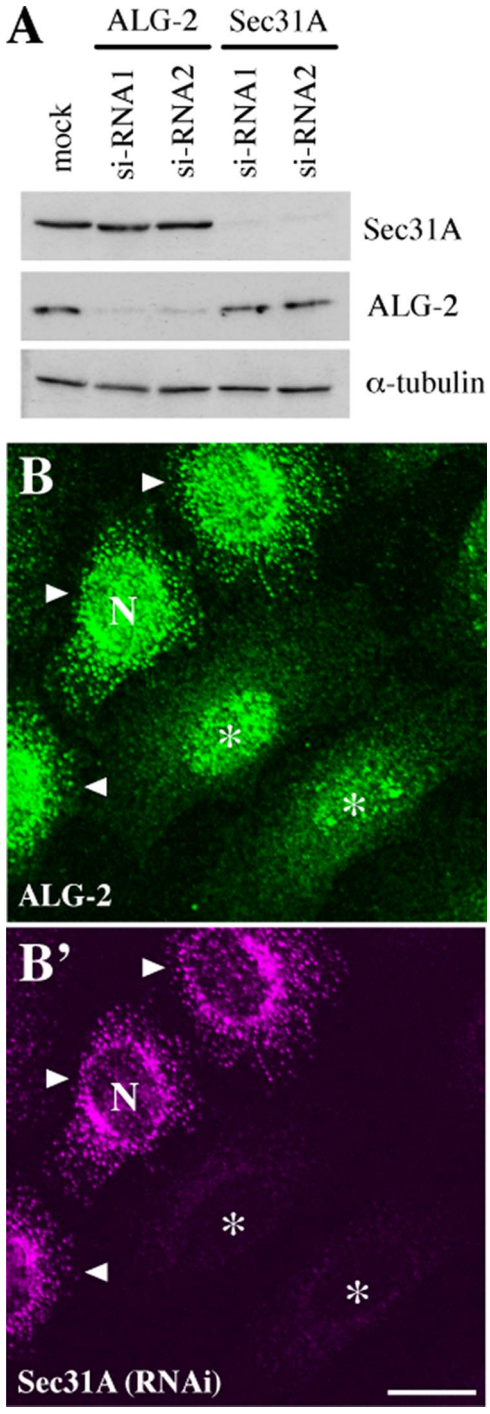

Figure 6. Depletion of Sec31A causes the mislocalization of ALG-2. (A) Lysates of HeLa cells transfected with the mock, two ALG-2 siRNA, and two Sec31A siRNA expression vectors were immunoblotted with anti-Sec31A (top), anti-ALG-2 (middle), and anti-α-tubulin (bottom) antibodies. (B and B′) HeLa cells were transfected with the Sec31A siRNA vector (S-siRNA1), and double stained with anti-ALG-2 (B) and anti-Sec31A (B′) antibodies. Asterisks and arrowheads indicate Sec31A-depleted and undepleted cells, respectively. N indicates nuclei. Bars, 20 μm.

(Figure 7 A and A′, asterisks; our unpublished data). Again, a field including both ALG-2–depleted and undepleted cells is intentionally shown in Figure 7, A and A′. These results suggested that ALG-2 is required for the maximal localiza-

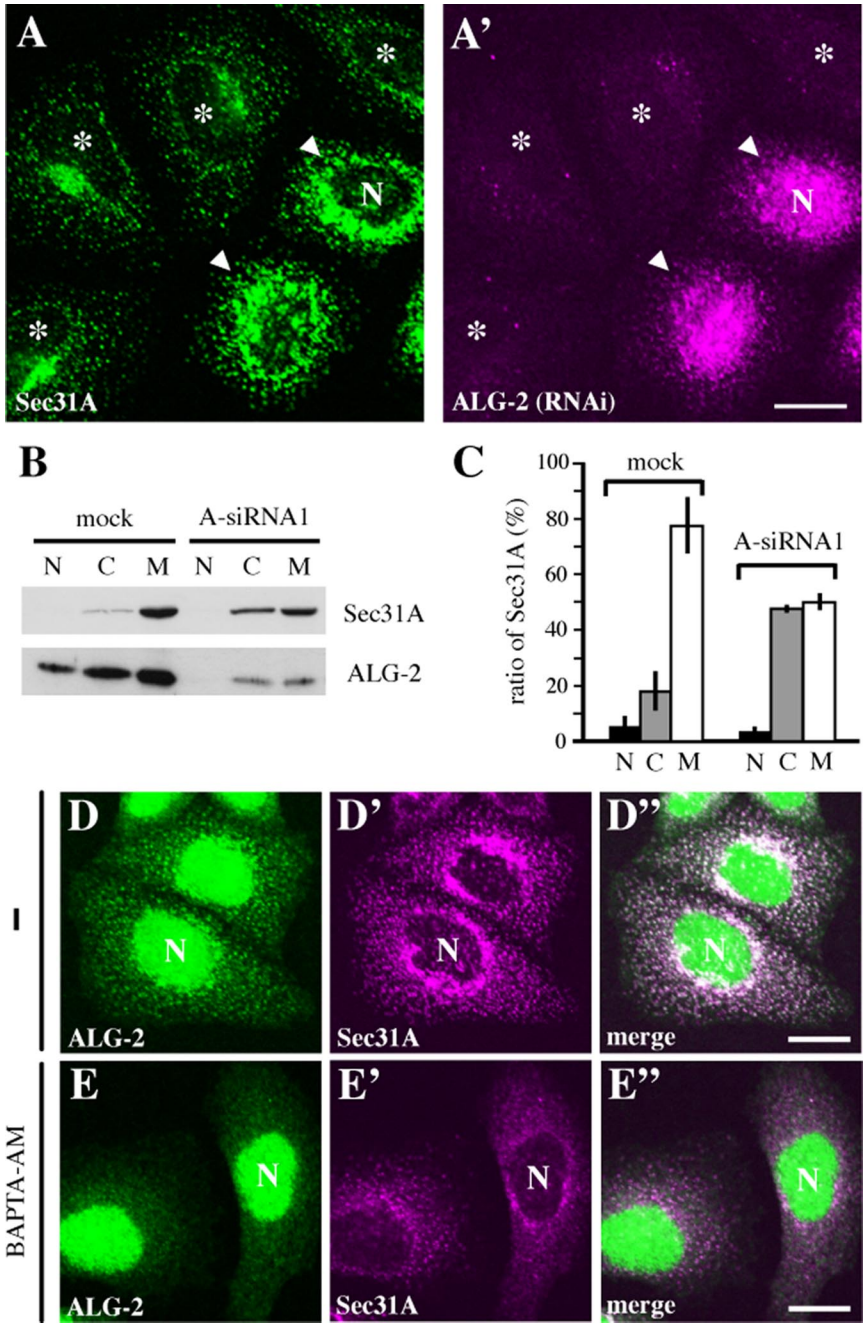

Figure 7. ALG-2 stabilizes the localization of Sec31A at ER exit sites. (A and A′) HeLa cells were transfected with the ALG-2 siRNA vector (A-siRNA1), and double stained with anti-Sec31A (A) and anti-ALG-2 (A′) antibodies. Asterisks and arrowheads indicate ALG-2–depleted and undepleted cells, respectively. (B) HeLa cells transfected with the mock or A-siRNA1 vector were homogenized and fractionated into nuclear (N), cytoplasmic (C), and membrane (M) fractions. Proteins in each fraction were immunoblotted with antibodies against Sec31A (top) and ALG-2 (bottom). (C) The experiment shown in B was repeated four times, and the intensity of the Sec31A band in each fraction was quantified. The mean ± SD of the Sec31A ratio (%) in each fraction is shown. (D–E″) HeLa cells were treated without (D–D″) or with (E–E″) BAPTA-AM and double stained with anti-ALG-2 (D and E) and anti-Sec31A (D′ and E′) antibodies. D″ and E″ are merged images. N indicates nuclei. Bars, 20 μm.

tion of Sec31A to ER exit sites. Similar to the ALG-2 level in Sec31A-depleted cells, the total cellular level of Sec31A was unchanged by ALG-2 depletion (Figure 6A, top). The level of p125, an ER exit site-localizing protein for which a mouse monoclonal antibody was available (Shimoi *et al*., 2005), was unchanged at ER exit sites by ALG-2 depletion (Supplemental Figure S2, A and A′).

We next examined the Sec31A association with the membrane in ALG-2–depleted cells by subcellular fractionation. Whereas Sec31A was largely distributed to the membrane fraction in mock-transfected cells, the Sec31A level in the cytoplasmic fraction was nearly equal to that in the membrane fraction in A-siRNA1– and A-siRNA2–transfected cells (Figure 7B, top; our unpublished data). The level of Sec31A recovered in the nuclear fraction was very low both in control and in ALG-2–depleted cells (Figure 7B). Quantification of the intensity of bands corresponding to Sec31A revealed that in mock-transfected cells, 5 ± 4, 18 ± 7, and 77 ± 10% of Sec31A were recovered in the nuclear, cytoplasmic, and membrane fractions, respectively (n = 4; Figure 7C). In ALG-2–depleted cells, by contrast, 3 ± 2, 47 ± 1, and 50 ± 3% were recovered in the nuclear, cytoplasmic, and membrane fractions, respectively (n = 4; Figure 7C).

Finally, we examined the effect of a cell-permeable Ca^{2+} chelator, BAPTA-AM, on the subcellular localization of ALG-2 and Sec31A. BAPTA-AM has been used to investigate the role of Ca^{2+} in various membrane traffic processes, including that between the ER and the Golgi (Ahluwalia *et al*., 2001; Chen *et al*., 2002), in living cells. After treatment of HeLa cells with 25 μM BAPTA-AM for 30 min, the punctate

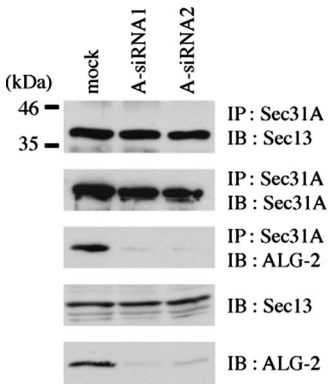

Figure 8. ALG-2 does not regulate the Sec13-Sec31A interaction. Lysates of HeLa cells transfected with the mock, A-siRNA1, and A-siRNA2 vectors were immunoprecipitated with anti-Sec31A antibody, and the precipitates were immunoblotted with anti-Sec13 (top), anti-Sec31A (second from the top), and anti-ALG-2 (third from the top) antibodies. The expression levels of Sec13 and ALG-2 were assessed by immunoblotting of the total cell lysates with anti-Sec13 (second from the bottom) and anti-ALG-2 (bottom) antibodies.

distribution of ALG-2 at ER exit sites was largely abolished (Figure 7E, compare with that in untreated cells in Figure 7D). Importantly, this was accompanied by a substantial reduction in the level of Sec31A at these sites (Figure 7E′, compare with Figure 7D′). By contrast, the level of p125 at ER exit sites was unaffected when the mislocalization of ALG-2 was induced by BAPTA-AM (Supplemental Figures S2, B–B″ and C–C″).

ALG-2 Does Not Regulate the Stability of the Sec13–Sec31A Complex

To test whether the ALG-2 binding to Sec31A regulates the Sec13–Sec31A complex formation, we examined the effect of ALG-2 depletion on Sec13 binding to Sec31A. Lysates of HeLa cells transfected with the mock, A-siRNA1, and A-siRNA2 expression vectors were immunoprecipitated with anti-Sec31A antibody. Immunoblotting of the precipitates with anti-Sec13 antibody showed that Sec13 was equally coprecipitated from mock- and ALG-2 siRNA–transfected cells (Figure 8, top). The level of cellular Sec13 was also unchanged by ALG-2 depletion (Figure 8, second panel from the bottom).

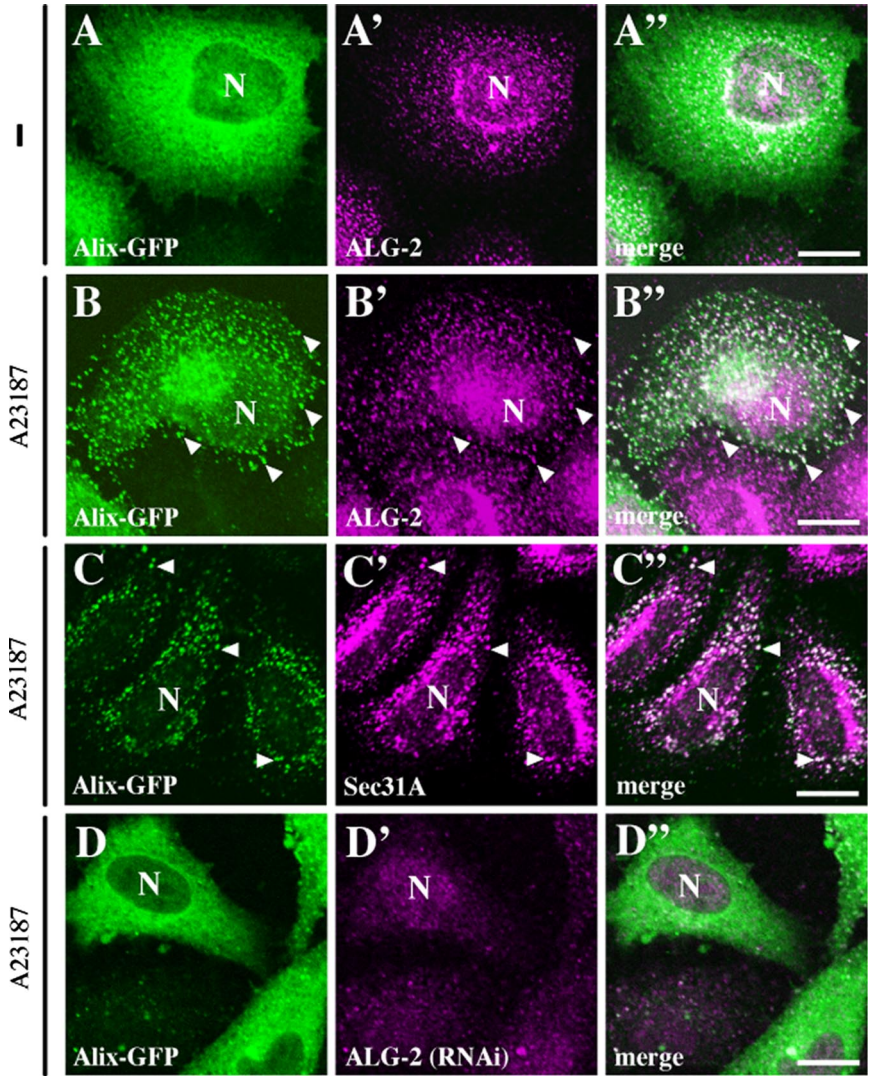

Figure 9. Alix is recruited to ER exit sites in an A23187- and ALG-2–dependent manner. (A–C″) HeLa cells were transfected with Alix-GFP, treated without (A–A″) or with (B–B″ and C–C″) A23187 and stained with anti-GFP antibody (A, B, and C) together with anti-ALG-2 (A′ and B′) or anti-Sec31A (C′) antibody. (D–D″) HeLa cells were cotransfected with Alix-GFP and the ALG-2 siRNA vector (A-siRNA1), treated with A23187, and double stained with anti-GFP (D) and anti-ALG-2 (D′) antibodies. A″, B″, C″, and D″ are merged images. Arrowheads indicate colocalization of Alix-GFP with ALG-2 (B–B″) and Sec31A (C–C″) in A23187-treated cells. N indicates nuclei. Bars, 20 μm.

ALG-2 Recruits Alix to ER Exit Sites in a Ca^{2+}-dependent Manner

ALG-2 binds Alix, an orthologue of the yeast class E Vps protein Bro1 (Missotten *et al*., 1999; Vito *et al*., 1999). We examined whether Alix colocalizes with ALG-2 at ER exit sites. When Alix was tagged at the C-terminal with GFP and expressed in HeLa cells, it exhibited a diffuse cytoplasmic distribution (Figure 9, A–A″), as reported previously for exogenously expressed Alix constructs (Chatellard-Causse *et al*., 2002; Katoh *et al*., 2003). Because the binding of Alix to ALG-2 is dependent on Ca^{2+}, we next tested whether increasing the intracellular Ca^{2+} concentration by using the Ca^{2+} ionophore A23187 induces the translocation of Alix-GFP. In cells treated with 1 μM A23187 for 20 min, Alix-GFP was detected on cytoplasmic punctate structures where it mostly colocalized with endogenous ALG-2 (Figure 9, B–B″) and Sec31A (Figure 9, C–C″), indicating that Alix-GFP localizes to ER exit sites in these cells. To examine whether ALG-2 is required for the recruitment of Alix, we tested the effect of ALG-2 depletion on the A23187-induced translocation of Alix-GFP. In cells transfected with A-siRNA1 or A-siRNA2, Alix-GFP retained a diffuse cytoplasmic distribution after A23187 treatment (Figure 9, D–D″; our unpublished data).

DISCUSSION

Binding of ALG-2 to Sec31A

The results of the GST pull-down and coimmunoprecipitation experiments showed that ALG-2 binds Sec31A (Figure 1). The binding was completely inhibited in the presence of EGTA (Figure 1), indicating that it is a Ca^{2+}-dependent interaction. Anti-ALG-2 antibody coprecipitated Sec31A from HeLa cell lysate in the absence of exogenously added Ca^{2+}, but the efficiency of the coprecipitation was increased by the addition of 10 μM Ca^{2+}. These results suggest that ALG-2 and Sec31A interact with each other at a physiological concentration of Ca^{2+} and that the interaction can be regulated by changes in the cytoplasmic Ca^{2+} level within the physiological range.

The binding of Ca^{2+} to ALG-2 induces a conformational change that allows ALG-2 to interact also with other proteins such as Alix (Missotten *et al*., 1999; Vito *et al*., 1999), annexins VII and XI (Satoh *et al*., 2002), and tumor susceptibility gene 101 (Katoh *et al*., 2005). Although the biological significance of these interactions remains unknown, the ALG-2–binding sites in these proteins are all located in Pro-rich regions (Satoh *et al*., 2002; Shibata *et al*., 2004; Katoh *et al*., 2005). We showed that ALG-2 binds to the Pro-rich region of Sec31A (Figure 2). Therefore, the mode of binding seems to be similar to that of other Ca^{2+}-dependent ALG-2-binding proteins and further supports the important role of Pro residues in Ca^{2+}-dependent interaction with ALG-2.

Mammalian genomes encode a second yeast Sec31 homologue termed Sec31B (Tang *et al*., 2000; Stankewich *et al*., 2006). Sec31B also harbors a Pro-rich region in the C-terminal region, although the amino acid sequence in this region is not highly conserved between Sec31A and Sec31B (~17%). Using the GST-ALG-2 fusion protein, however, we were not able to pull down Sec31B as a major ALG-2–binding protein from HeLa cells (Figure 1), raising the possibility that ALG-2 does not bind Sec31B. Another possibility is that Sec31B is not expressed in HeLa cells or expressed at a much lower level than Sec31A, which is consistent with the predominant expression of the *Sec31B* gene in the testis (Tang *et al*., 2000; Stankewich *et al*., 2006). Therefore, whether ALG-2 also binds Sec31B remains to be tested.

Localization of ALG-2 to ER Exit Sites

Previous immunofluorescence experiments have suggested the localization of ALG-2 in the nucleus and cytoplasm (Kitaura *et al*., 2001). In this study, however, we found that ALG-2 is distributed to cytoplasmic puncta where it colocalizes with markers for ER exit sites such as Sec31A and p125 (Figures 3 and 4). The localization of ALG-2 was unchanged by treatment with BFA, which inactivates the small GTPase Arf1 and causes the redistribution of Golgi proteins to the ER without affecting the morphology or protein composition of ER exit sites (Figure 4; Klausner *et al*., 1992; Ward *et al*., 2001). By contrast, the distribution of ALG-2 was affected in the same manner as that of Sec31A when the function of Sar1, a small GTPase that recruits the COPII components to ER exit sites, was dysregulated by the overexpression of its GTP- and GDP-locked mutants (Figure 4). We also showed by subcellular fractionation experiments that ALG-2 is recovered in the membrane fraction in addition to the nuclear and cytoplasmic fractions (Figure 3). Together, these results indicate that the ER exit site is at least one of the major sites of the localization and action of ALG-2 within cells.

Several evidence indicate that Sec31A recruits ALG-2 to ER exit sites. First, ALG-$2^{E47/114A}$, a mutant that is unable to bind Ca^{2+} and therefore do not bind Sec31A (Figure 1), did not localize to ER exit sites unlike wild-type protein when exogenously expressed (Figure 5). Second, overexpression of the Pro-rich region of Sec31A, which binds ALG-2 but cannot localize to ER exit sites, abolished the ALG-2 localization (Figure 5). Third, depletion of Sec31A by using RNAi resulted in almost the complete disappearance of ALG-2 from ER exit sites without a change in the cellular level of the protein (Figure 6). Finally, treatment of cells with a Ca^{2+} chelator BAPTA-AM abolished the normal punctate localization of ALG-2 (Figure 7). Based on these results, we conclude that ALG-2 is recruited to ER exit sites via Ca^{2+}-dependent interaction with Sec31A. The mislocalization of ALG-2 in Sec31A-depleted cells also suggests that Sec31B, regardless of whether it is expressed in HeLa cells, is not responsible for the ALG-2 localization at ER exit sites in these cells.

Role of ALG-2 at ER Exit Sites

Immunofluorescence staining experiments showed that the Sec31A level at ER exit sites was substantially reduced, but not abolished, in cells depleted of ALG-2 (Figure 7). By subcellular fractionation, Sec31A was redistributed from the membrane to the cytoplasmic fraction when cellular ALG-2 was depleted (Figure 7). Finally, the level of Sec31A was also reduced when ALG-2 was mislocalized from ER exit sites by treating cells with BAPTA-AM (Figure 7). Together, we suggest that ALG-2 does not play a role in the recruitment of Sec31A to ER exit sites but that it stabilizes its localization at these sites. We were not able to examine the effect of ALG-2 depletion on the levels of other COPII components at ER exit sites because available antibodies for these proteins were all of rabbit origin. This precluded us from distinguishing between ALG-2–depleted and undepleted cells by costaining Sec13- and Sec23-labeled cells with our rabbit polyclonal anti-ALG-2. Instead, we examined p125, a protein that solely localizes to ER exit sites via Sec23 (Shimoi et al., 2005), by using mouse monoclonal anti-p125 antibody. The pattern of anti-p125 staining was unaffected by ALG-2 depletion or by incubation with BAPTA-AM (Supplemental Figure S2), suggesting that ALG-2 does not regulate the localization of Sec23 at ER exit sites. We therefore speculate that ALG-2

specifically regulates the function of Sec31A without influencing the entire structure of ER exit sites. Formation of the Sec13–Sec31A outer shell complex was also unaffected by ALG-2 depletion (Figure 8). Therefore, the binding of ALG-2 may change the conformation of Sec31A, which leads to greater binding affinity of the Sec13–Sec31A complex to the Sec23–Sec24 inner shell complex.

VSV-045G, a temperature-sensitive mutant of the vesicular stomatitis virus G protein (VSVG; Gallione and Rose 1985), is a cargo commonly used to test ER-to-Golgi vesicular traffic. We examined the effect of RNAi-mediated ALG-2 depletion on the transport of VSV-045G from the ER in HeLa cells. We, however, were not able to find detectable difference by immunofluorescence in the rate of ER-to-Golgi trafficking of VSVG between control and ALG-2–depleted cells at a permissive temperature (our unpublished data). In the same experimental conditions, overexpression of $Sar1^{H79G}$ or $Sar1^{T39N}$ totally blocked the traffic (our unpublished data). One explanation for this observation is that for the transport of VSVG in this assay, the residual Sec31A level at ER exit sites is sufficient for the formation of COPII-coated vesicles in ALG-2–depleted cells. Another possibility is that Sec31B, if expressed in HeLa cells, may compensate for the reduced level of Sec31A in these cells.

COPII coat-dependent vesicular transport is conserved from yeasts to humans, raising the question of whether the regulation of the COPII coat by ALG-2 is conserved in yeast cells. The *S. cerevisiae* genome encodes a single PEF family protein YGR058w, the function of which has not been determined (Maki *et al*., 2002). Although YGR058w shares ~28% amino acid sequence identity with mammalian ALG-2 in the PEF domain, it contains an N-terminally located additional ~160 amino acid region that is lacking in ALG-2. Therefore, it is of interest to test whether YGR058w binds Sec31 and participates in the Ca^{2+}-mediated regulation of COPII-dependent vesicular traffic in yeast cells.

Does Alix Play a Role at ER Exit Sites?

Alix is a mammalian orthologue of the class E Vps protein Bro1 in *S. cerevisiae*. Liposomes containing lysobisphosphatidic acid (LBPA), an unconventional phospholipid enriched in the membrane of MVB vesicles (Kobayashi *et al*., 1998), spontaneously form internal vesicles when their lumen is mildly acidic (Matsuo *et al*., 2004). Alix binds to LBPA-containing liposomes and inhibits the formation of the internal vesicles in vitro (Matsuo *et al*., 2004). In addition, RNAi-mediated depletion of Alix in mammalian cells results in a reduction in the number of multilamellar late endosomes and the LBPA level in the organelle (Matsuo *et al*., 2004). These results suggest an essential role for Alix in the biogenesis of MVBs. Although Alix was originally identified as a protein that binds ALG-2 (Missotten *et al*., 1999; Vito *et al*., 1999), the biological significance of this interaction has been unclear. In this study, we showed that the treatment of cells expressing GFP-tagged Alix with the Ca^{2+} ionophore A23187 induces the translocation of the Alix protein to ER exit sites from the cytoplasm (Figure 9). This process was inhibited when cellular ALG-2 was depleted by using RNAi (Figure 9), suggesting that ALG-2 recruits Alix to ER exit sites via a direct Ca^{2+}-dependent interaction. We cannot exclude the possibility that the translocation of Alix is an artificial phenomenon that is only observed in cells overexpressing Alix and treated with a powerful Ca^{2+} ionophore, A23187. It is therefore important to examine whether endogenous Alix is translocated to ER exit sites in response to a physiological stimulation that elevates the cytoplasmic Ca^{2+} level. Nonetheless, our findings suggest for the first time a possible novel function of Alix at ER exit sites. This issue must be explored in future studies.

Regulation of ER-to-Golgi trafficking by Ca^{2+}

Evidence has accumulated that Ca^{2+} plays essential roles in vesicular traffic between the ER and the Golgi (Beckers and Balch, 1989; Pind *et al*., 1994; Ivessa *et al*., 1995; Ahluwalia *et al*., 2001; Chen *et al*., 2002; Hasdemir *et al*., 2005). Consistent with this, both the ER and the Golgi are intracellular Ca^{2+} stores (Pinton *et al*., 1998; Petersen *et al*., 2001), and the cytoplasmic Ca^{2+} concentration is reported to be relatively high around these organelles (Wahl *et al*., 1992). However, Ca^{2+}-binding proteins of which functions are directly regulated by Ca^{2+} in this trafficking pathway have been mostly unidentified. Moreover, the involvement of Ca^{2+} in the regulation of the COPII coat function has not been suggested. Therefore, our results demonstrating that ALG-2 stabilizes the Sec31A localization at ER exit sites provide a novel Ca^{2+}-dependent regulatory mechanism in the early stage of ER-to-Golgi anterograde traffic.

ACKNOWLEDGMENTS

We thank Dr. Hong for the anti-Sec13 antibody, Drs. Maki and Shibata for the ALG-2 and Alix expression constructs, Dr. Tagaya (Tokyo University of Pharmacy and Life Science, Hachioji, Japan) for discussion and critical reading of the manuscript, and Dr. Kakiyama for technical assistance with the mass spectrometry analysis. This work was supported by Grants-in-Aid 17370045 (to N.K.) and 17570156 and 18050011 (to M.K.) from the Ministry of Education, Culture, Sports, Science, and Technology of Japan and a research grant from the Kato Memorial Bioscience Foundation (to M.K.).

REFERENCES

Ahluwalia, J. P., Topp, J. D., Weirather, K., Zimmerman, M., and Stamnes, M. (2001). A role for calcium in stabilizing transport vesicle coats. J. Biol. Chem. *276*, 34148–34155.

Barlowe, C., Orci, L., Yeung, T., Hosobuchi, M., Hamamoto, S., Salama, N., Rexach, M. F., Ravazzola, M., Amherdt, M., and Schekman, R. (1994). COPII: a membrane coat formed by Sec proteins that drive vesicle budding from the endoplasmic reticulum. Cell *77*, 895–907.

Barlowe, C., and Schekman, R. (1993). SEC12 encodes a guanine-nucleotide-exchange factor essential for transport vesicle budding from the ER. Nature *365*, 347–349.

Beckers, C.J.M., and Balch, W. E. (1989). Calcium and GTP: essential components in vesicular trafficking between the endoplasmic reticulum and Golgi apparatus. J. Cell Biol. *108*, 1245–1256.

Chatellard-Causse, C., Blot, B., Cristina, N., Torch, S., Missotten, M., and Sadoul, R. (2002). Alix (ALG–2-interacting protein X), a protein involved in apoptosis, binds to endophilins and induces cytoplasmic vacuolization. J. Biol. Chem. *277*, 29108–29115.

Chen, J.-L., Ahluwalia, J. P., and Stamnes, M. (2002). Selective effects of calcium chelators on anterograde and retrograde protein transport in the cell. J. Biol. Chem. *277*, 35682–35687.

Forster, R., Weiss, M., Zimmermann, T., Reynaud, E. G., Verissimo, F., Stephens, D. J., and Pepperkok, R. (2006). Secretory cargo regulates the turnover of COPII subunits at single ER exit sites. Curr. Biol. *16*, 173–179.

Gallione, C. J., and Rose, J. K. (1985). A single amino acid substitution in a hydrophobic domain causes temperature-sensitive cell-surface transport of a mutant viral glycoprotein. J. Virol. *54*, 374–382.

Hasdemir, B., Fitzgerald, D. J., Prior, I. A., Tepikin, A. V., and Robert D. Burgoyne, R. D. (2005). Traffic of Kv4 K^+ channels mediated by KChIP1 is via a novel post-ER vesicular pathway. J. Cell Biol. *171*, 459–469.

Hicke, L., Yoshihisa, T., and Schekman, R. (1992). Sec23p and a novel 105-kDa protein function as a multimeric complex to promote vesicle budding and protein transport from the endoplasmic reticulum. Mol. Biol. Cell *3*, 667–676.

Ivessa, N. E., De Lemos-Chiarandini, C., Gravotta, D., Sabatini, D. D., and Kreibich, G. (1995). The brefeldin A-induced retrograde transport from the Golgi apparatus to the endoplasmic reticulum depends on calcium sequestered to intracellular stores. J. Biol. Chem. *270*, 25960–25967.

Katoh, K., Shibata, H., Suzuki, H., Nara, A., Ishidoh, K., Kominami, E., Yoshimori, T., and Maki, M. (2003). The ALG-2-interacting protein Alix associates with CHMP4b, a human homologue of yeast Snf7 that is involved in multivesicular body sorting. J. Biol. Chem. *278*, 39104–39113.

Katoh, K., Suzuki, H., Terasawa, Y., Mizuno, T., Yasuda, J., Shibata, H., and Maki, M. (2005). The penta-EF-hand protein ALG-2 directly interacts with the ESCRT-I component TSG101 and Ca^{2+}-dependently colocalizes to aberrant endosomes with dominant-negative AAA ATPase SKD1/Vps4B. Biochem J. *391*, 677–685.

Kitaura, Y., Matsumoto, S., Satoh, H., Hitomi, K., and Maki, M. (2001). Peflin and ALG-2, members of the penta-EF-hand protein family, form a heterodimer that dissociates in a Ca^{2+}-dependent manner. J. Biol. Chem. *276*, 14053–14058.

Klausner, R. D., Donaldson, J. G., and Lippincott-Schwartz, J. (1992). Brefeldin A: insights into the control of membrane traffic and organelle structure. J. Cell Biol. *116*, 1071–1080.

Kobayashi, T., Stang, E., Fang, K. S., de Moerloose, P., Parton, R. G., and Gruenberg, J. (1998). A lipid associated with the antiphospholipid syndrome regulates endosome structure and function. Nature *392*, 193–197.

Kuehn, M. J., Herrmann, J. M., and Schekman, R. (1998). COPII-cargo interactions direct protein sorting into ER-derived transport vesicles. Nature *391*, 187–190.

Lo, K.W.-H., Zhang, Q., Li, M., and Zhang, M. (1999). Apoptosis-linked gene product ALG-2 is a new member of the calpain small subunit subfamily of Ca^{2+}-binding proteins. Biochemistry *38*, 7498–7508.

Maki, M., Kitaura, Y., Satoh, H., Ohkouchi, S., and Shibata, H. (2002). Structures, functions and molecular evolution of the penta-EF-hand Ca^{2+}-binding proteins. Biochim. Biophys. Acta *1600*, 51–60.

Maki, M., Yamaguchi, K., Kitaura, Y., Satoh, H., and Hitomi, K. (1998). Calcium-induced exposure of a hydrophobic surface of mouse ALG-2, which is a member of the penta-EF-hand protein family. J. Biochem. *124*, 1170–1177.

Matsuo, H., *et al*. (2004). Role of LBPA and Alix in multivesicular liposome formation and endosome organization. Science *303*, 531–534.

Matsuoka, K., Orci, L., Amherdt, M., Bednarek, S. Y., Hamamoto, S., Schekman, R., and Yeung, T. (1998). COPII-coated vesicle formation reconstituted with purified coat proteins and chemically defined liposomes. Cell *93*, 263–275.

Missotten, M., Nichols, A., Rieger, K., and Sadoul, R. (1999). Alix, a novel mouse protein undergoing calcium-dependent interaction with the apoptosis-linked gene 2 (ALG-2) protein. Cell Death Differ. *6*, 124–129.

Mizuno, E., Kawahata, K., Kato, M., Kitamura, N., and Komada, M. (2003). STAM proteins bind ubiquitinated proteins on the early endosome via the VHS domain and ubiquitin-interacting motif. Mol. Biol. Cell *14*, 3675–3689.

Nakano, A., and Muramatsu, M. (1989). A novel GTP-binding protein, Sar1p, is involved in transport from the endoplasmic reticulum to the Golgi apparatus. J. Cell Biol. *109*, 2677–2691.

Petersen, O. H., Tepikin, A., and Park, M. K. (2001). The endoplasmic reticulum: one continuous or several separate Ca^{2+} stores? Trends Neurosci. *24*, 271–276.

Pind, S. N., Nuoffer, C., McCaffery, J. M., Plutner, H., Davidson, H. W., Farquhar, M. G., and Balch, W. M. (1994). Rab1 and Ca^{2+} are required for the fusion of carrier vesicles mediating endoplasmic reticulum to Golgi transport. J. Cell Biol. *125*, 239–252.

Pinton, P., Pozzan, T., and Rizzuto, R. (1998). The Golgi apparatus is an inositol 1,4,5-trisphosphate-sensitive Ca^{2+} store, with functional properties distinct from those of the endoplasmic reticulum. EMBO J. *17*, 5298–5308.

Salama, N. R., Yeung, T., and Schekman, R. W. (1993). The Sec13p complex and reconstitution of vesicle budding from the ER with purified cytosolic proteins. EMBO J. *12*, 4073–4082.

Satoh, H., Nakano, Y., Shibata, H., and Maki, M. (2002). The penta-EF-hand domain of ALG-2 interacts with amino-terminal domains of both annexin VII and annexin XI in a Ca^{2+}-dependent manner. Biochim. Biophys. Acta *1600*, 61–67.

Shibata, H., Yamada, K., Mizuno, T., Yorikawa, C., Takahashi, H., Satoh, H., Kitaura, Y., and Maki, M. (2004). The penta-EF-hand protein ALG-2 interacts with a region containing PxY repeats in Alix/AIP1, which is required for the subcellular punctate distribution of the amino-terminal truncation form of Alix/AIP1. J. Biochem. *135*, 117–128.

Shimoi, W., Ezawa, I., Nakamoto, K., Uesaki, S., Gabreski, G., Aridor, M., Yamamoto, A., Nagahama, M., Tagaya, M., and Tani, K. (2005). p125 is localized in endoplasmic reticulum exit sites and involved in their organization. J. Biol. Chem. *280*, 10141–10148.

Shugrue, C. A., Kolen, E. R., Peters, H., Czernik, A., Kaiser, C., Matovcik, L., Hubbard, A. L., and Gorelick, F. (1999). Identification of the putative mammalian orthologue of Sec31p, a component of the COPII coat. J. Cell Sci. *112*, 4547–4556.

Stagg, S. M., Gurkan, C., Fowler, D. M., LaPointe, P., Foss, T. R., Potter, C. S., Carragher, B., and Balch, W. E. (2006). Structure of the Sec13/31 COPII coat cage. Nature *439*, 234–238.

Stankewich, M. C., Stabach, P. R., and Morrow, J. S. (2006). Human Sec31B: a family of new mammalian orthologues of yeast Sec31p that associate with the COPII coat. J. Cell Sci. *119*, 958–969.

Strack, B., Calistri, A., Craig, S., Popova, E., and Gottlinger, H. G. (2003). AIP1/Alix is a binding partner for HIV-1 p6 and EIAV p9 functioning in virus budding. Cell *114*, 689–699.

Tang, B. L., Peter, F., Krijnse-Locker, J., Low, S. H., Griffiths, G., and Hong, W. (1997). The mammalian homolog of yeast Sec13p is enriched in the intermediate compartment and is essential for protein transport from the endoplasmic reticulum to the Golgi apparatus. Mol. Cell Biol. *17*, 256–266.

Tang, B. L., Wang, Y., Ong, Y. S., and Hong, W. (2005). COPII and exit from the endoplasmic reticulum. Biochim. Biophys. Acta *1744*, 304–315.

Tang, B. L., Zhang, T., Low, D.Y.H., Wong, E. T., Horstmann, H., and Hong, W. (2000). Mammalian homologues of yeast Sec31p. J. Biol. Chem. *275*, 13597–13604.

Tani, K., Mizoguchi, T., Iwamatsu, A., Hatsuzawa, K., and Tagaya, M. (1999). p125 is a novel mammalian Sec23p-interacting protein with structural similarity to phospholipid-modifying proteins. J. Biol. Chem. *274*, 20505–20512.

Tarabykina, S., Mollerup, J., Winding, P., and Berchtold, M. W. (2004). ALG-2, a multifunctional calcium binding protein? Front. Biosci. *9*, 1817–1832.

Vito, P., Lacana, E., and D'Adamio, L. (1996). Interfering with apoptosis: Ca^{2+}-binding protein ALG-2 and Alzheimer's disease gene ALG-3. Science *271*, 521–525.

Vito, P., Pellegrini, L., Guiet, C., and D'Adamio, L. (1999). Cloning of AIP1, a novel protein that associates with the apoptosis-linked gene ALG-2 in a Ca^{2+}-dependent reaction. J. Biol. Chem. *274*, 1533–1540.

von Schwedler, U. K., *et al*. (2003). The protein network of HIV budding. Cell *114*, 701–713.

Wahl, M., Sleight, R. G., and Gruenstein, E. (1992). Association of cytoplasmic free Ca^{2+} gradients with subcellular organelles. J. Cell Physiol. *150*, 593–609.

Ward, T. H., Polishchuk, R. S., Caplan, S., Hirschberg, K., and Lippincott-Schwartz, J. (2001). Maintenance of Golgi structure and function depends on the integrity of ER export. J. Cell Biol. *155*, 557–570.

Watson, P., and Stephens, D. J. (2005). ER-to-Golgi transport: form and formation of vesicular and tubular carriers. Biochim. Biophys. Acta *1744*, 304–315.

Yoshihisa, T., Barlowe, C., and Schekman, R. (1993). Requirement for a GTPase-activating protein in vesicle budding from the endoplasmic reticulum. Science *259*, 1466–1468.